e-ISSN 2083–4640
ISSN 1507–1367

RESEARCH PAPER

Reports of Practical Oncology and Radiotherapy
2021, Volume 26, Number 4, pages: 590–597
DOI: 10.5603/RPOR.a2021.0083
Submitted: 22.09.2020
Accepted: 27.02.2021

Dosimetric study of Hounsfield number correction effect in areas influenced by contrast product in lungs case

Yassine Oulhouq[1,3], Dikra Bakari[2], Deae-Eddine Krim[1], Mustapha Zerfaoui[1], Abdeslem Rrhioua[1], Soufiane Berhili[3], Loubna Mezouar[3]

[1]LPMR, Faculty of Sciences, University Mohamed 1st, Oujda, Morocco
[2]National School of Applied Sciences, University Mohamed 1st, Oujda, Morocco
[3]HASSAN II Oncology Center, University Hospital Mohammed VI, Oujda, Morocco

ABSTRACT

Background: The aim of the study was dosimetric effect quantification of exclusive computed tomography (CT) use with an intravenous (IV) contrast agent (CA), on dose distribution of 3D-CRT treatment plans for lung cancer. Furthermore, dosimetric advantage investigation of manually contrast-enhanced region overriding, especially the heart.

Materials and methods: Ten patients with lung cancer were considered. For each patient two planning CT sets were initially taken with and without CA. Treatment planning were optimized based on CT scans without CA. All plans were copied and recomputed on scans with CA. In addition, scans with IV contrast were copied and density correction was performed for heart contrast enhanced. Same plans were copied and replaced to undo dose calculation errors that may be caused by CA. Eventually, dosimetric evaluations based on dose volume histograms (DVHs) of planning target volumes (PTV) and organs at-risk were studied and analyzed using the Wilcoxon's signed rank test.

Results: There is no statistically significant difference in dose calculation for the PTV maximum, mean, minimum doses, spinal cord maximum doses and lung volumes that received 20 and 30 Gy, between planes calculated with and without contrast scans ($p > 0.05$) and also for contrast scan, with manual regions overriding.

Conclusions: Dose difference caused by the contrast agent is negligible and not significant. Therefore, there is no justification to perform two scans, and using an IV contrast enhanced scan for dose calculation is sufficient.

Key words: lung cancer; contrast agent; tomography; 3D-CRT; PTV; dose calculation

Rep Pract Oncol Radiother 2021;26(4):590–597

Introduction

In lung radiation therapy, the purpose of the planning CT scans, is to set up the patient in the treatment position and obtain CT images that simulate patient's exact anatomical position during treatment to allow precise treatment planning [1].

Accurate segmentation of the normal tissue and tumor is necessary for good tumor treatment and reducing delivered dose to normal tissue all around tumor [2–4].

Many studies presented the benefit of using 4D simulation over 3D simulation in decreasing the PTV with possibly more benefit for smaller size tumors, peripherally located tumors, lower lobe tumors [5], and to define the respiration-induced tumor movement for the VMAT treatment [6]. In addition, using four-dimensional CT (4D-CT) can

Address for correspondence: Deae-Eddine Krim, Physics Department Laboratory of Physics of Matter and Radiations Faculty of Sciences, University Mohammed First Oujda Morocco Bvd Mohamed VI, Oujda, tel: +212 636 866 627 ; e-mail: d.krim@ump.ac.ma

help to reduce radiation damage to the surrounding organ at risk (OAR) [7].

The accessibility to these modern imaging (4D-CT) and treatment (VMAT) techniques is not equitably offered to all lung cancer patients worldwide, mainly because of logistic and economic inter-regional disparities.

For example, in Africa, most radiotherapy centers are fairly basic. They mostly offer palliative services and simple curative treatments based on two-dimensional imaging and treatment planning. Approximately 80% of centers are small, with one or two radiotherapy machines and basic equipment for imaging and treatment planning. Some advanced centers are equipped with modern imaging tools, treatment systems and more complex radiotherapy procedures such as three-dimensional conformal radiotherapy. These centers are able to perform intensity-modulated radiotherapy and image-guided procedures. However, the latter account for only about 2% of radiotherapy centers in Africa[8].

Hence, in this study, the focus will be put on the 3D-CRT treatment. Thus, the majority of lung cancer treatments is done by the 3DCRT technique.

In three-dimensional conformal radiotherapy, CT images are used for creating three-dimensional graphics. Hounsfield Units (HU) of CT images are used as the basis for dose calculation and heterogeneity correction. CT scans may be performed with or without CA.

However, using iodine contrast-enhanced computed tomography in the treatment planning for thoracic radiation therapy, more accurate delineation of tumor and lymph nodes is attained than when non contrast-enhanced images are used for contouring. Since contrast agent helps define the planning target volume (PTV) and organ at risk region very precisely, some studies have recommended intravenous CA use for planning CT scans [9–11].

Iodine CA, used in CT imaging, increases HU in tissue and becomes high density tissue for dose calculation [12, 13].

However, CA following a CT scan is excreted in urine, so it is only present during the CT acquisition process, and not during treatment. This may result in changes to patient delivered dose if dosimetric simulation uses CT images with a CA.

Currently, the practice of radiation therapy for lung cancer is to obtain two CT scans for the same patient, the first scan is performed without injection of CA, while the second one is carried out with the injection. This method was designed to incorporate benefits of intravenous contrast for visualizing anatomy while reducing perceived errors in dose calculations that may be caused by the injection of CA.

The two scans (without and with CA) are fused and contouring of tumor volumes and organs at risk is done using an IV contrast scan. These two scans are then separated, and the planning is done only on scanner without contrast. Though, respiratory motion could influence the fusion's precision between the two scans.

However, in order to perform the simulation following this protocol, the patient must receive double exposure to radiation caused by CT scan.

In this task, firstly we quantified and evaluated the dosimetric effects of using a contrast agent in the simulation of the treatment on CT scans, through complete dosimetric plans comparison between the two CT scans with and without a contrast agent. Secondly, we study the effect of a manual correction of Hounsfield unit on regions with contrast, especially heart, by replacing density of these highlighted region with the mean value of Hounsfield unit of the same regions in absence of contrast. The goal is to compare the reference plan, that we define as the plan computed in non-contrasted scans, with both dosimetric plans calculated with contrast scan and with contrast corrected.

Materials and methods

In this task, ten patients with lung cancer are considered. A treatment planning study was conducted to assess the effect of intravenous AC, during CT planning, on the radiation dose distribution of 3DCRT plans.

CT scanner data for each patient were performed using a General Electrical Medical Systems (OPTIMA CT 580) scanner with a slice thickness of 3 mm. In addition, patients were positioned supine, with both arms raised to top of the head on a pulmonary board designed to immobilize the patient. An initial isocenter was selected using scanner's lasers. This position was marked on the patient with a skin tattoo.

Two planning CTs sets that covered the total thorax volume were initially taken with and without intravenous CA.

Contrast-less CT and contrast-enhanced CT scans were acquired with the same scan protocol, but with a delay of 50 s after injection of iodine contrast at 2 mL/s rate, for contrast CT scan.

After CT scans acquisition, data were transferred to the treatment planning system Eclipse 13.6 through network. The two CT scans, with and without IV contrast, were fused together using fusion option in the Eclipse TPS.

The target volumes were contoured by medical physicians on CTs with a contrast agent. Where the GTV was defined as solid abnormality on CT. Subsequently, CTV was given as a 10 mm margin around the GTV, in which both the primary tumor site and levels of lymph nodes, to which the enlarged lymph nodes belonged, were involved. Remember that PTV is defined as CTV plus a 3 to 5 mm margin and that organs at risk include the heart, normal lungs and spinal cord.

Target contours and OARs have been copied and transferred from Enhanced Contrast CT on a non-contrast scan and could be refined by referring to non-contrast CT scans.

The set of contrast-enhanced CTs with contours will be copied, to obtain two sets of CTs with a contrast agent. In this second copied series, heart HUs will be overridden using TPS Eclipse by the average HUs of the heart in the non-contrast CT. Thus, we will have three CT scans, one without contrast, the second one with contrast, and the third one modified CT with contrast [1]. An example of the difference between the three scans is shown in Figure 1.

The PTVs of patients are treated by dose of 66 Gy at 2 Gy/fraction daily. The planning objectives were to limit prescribed dose to at least 95% of PTV with maximum dose at 110% of prescribed dose. For all of these patient cases, planning was performed using multiple beams calculated using an AAA algorithm from Eclipse 13.6 Treatment Planning. Where beam weights, field-in-field technique and wedge angles were selected to improve dose coverage of the target volumes. Multi Leaf Collimators were used to protect OARs by minimizing the dose for the normal lungs [14] and heart.

For each patient, a non-contrast scan was used as the reference scan set for dosimetric calculations. Once the plan is complete, it will be saved as a template. Its parameters will be copied and applied to different data sets.

This reference plan template is copied and applied to contrast enhanced CT and contrast enhanced modified CT sets, with a re-optimization of the plan parameters, which included radiotherapy field sizes and leaf shapes.

To analyze the treatment plans, isodose curves, DVHs of PTV and OARs were compared between the three plans for each patient.

Maximum, minimum and mean dose of PTV, heterogeneity index (HI) and conformity index (CI) were basic comparison parameters.

HI and CI was defined according to RTOG definitions [15], and they are used to estimate the degree of congruence between tumor contour and healthy tissue contour isodoses through geometric intersection methods [15-18]. These quality indices are defined as follows:

$$HI = \frac{I_{\max}}{\mathrm{RI}} \quad (1)$$

$$CI = \frac{V_{\mathrm{RI}}}{\mathrm{TV}} \quad (2)$$

where I_{max} is the maximum dose in the PTV, RI is the reference isodose (95% of prescription dose, ICRU50), V_{RI} is the volume covered by the prescription isodose and TV is the target volume.

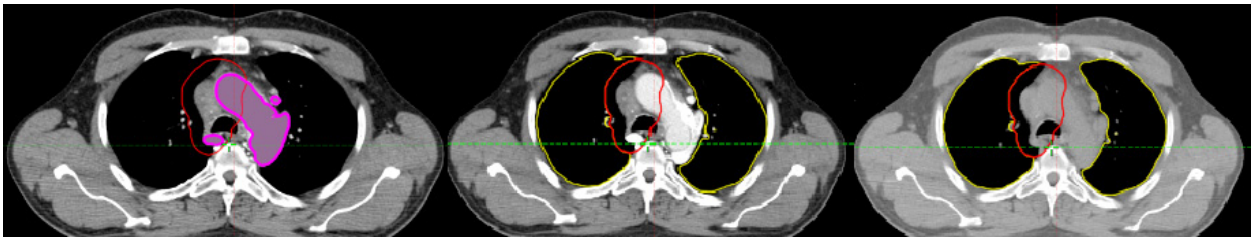

Figure 1. Right: contrast-less. Center: contrast-enhanced. Left: Modified contrast-enhanced CT scan

Moreover, the HI ideal value is 1 and increases as the plan becomes less homogeneous and the value less or equal to 2 is considered not to deviate from the RTOG recommendation [15]. Thereafter, the CI evaluates the conformity of reference isodose to the PTV, the CI equal to 1 relates to ideal conformity, and plans do not deviate from the RTOG recommendation if the CI value is between 1.0 and 2.0 [15].

Analysis of OARs for each patient included the percentage lung volumes which received 20 and 30 Gy (V20 and V30) to normal lung volume, respectively.

Wilcoxon sign rank test was utilized to analyze the differences. P-value less than 0.05 is considered statistically significant.

Results

Agreement between contours of contrast and non-contrast scans fused was assessed with Dice Similarity Coefficient (DSC) to quantify registration accuracy [19, 20].

DSC quantifies agreement between contours according to the degree of overlap of their volumes by using the following equation eq. 3.

$$DSC = \frac{V_d \cap V_m}{(V_d \cup V_m)/2} \quad (3)$$

Where V_d is the deformed volume and V_m is the reference volume. In our case V_m corresponds to the contour drawn on the non-contrast scan and V_d corresponds to the contour on the contrast scan fused.

Table 1. Dice similarity coefficient (DSC), of normal lungs (lungs-PTV)

	Normal lungs		
	Mean	SD	Range
DSC	0.93	0.059	0.8–0.96

Fusion accuracy for each patient was compared following recommendations set forth in the TG132 report, which recommends DSC between 0.8 and 0.9 [21–23].

For all patients, the accuracy of the fusion remained within tolerances recommended by TG132 (Dice similarity coefficient > 0.8). Example of DSC calculated for normal lungs was presented in Table 1.

3D-CRT main aim is to irradiate targets with 95% of prescribed dose. Tables 2 and 3 describe the comparison of PTV maximum, mean, and minimum doses of the contrast scan (C+) and the contrast scan with manual regions overriding (C + mdf), compared to the non-contrast plan (C–).

Regarding DVH curve (Fig. 2), it is observed that there are no notable changes between DVHs of the contrast scan and the contrast scan with regions processed manually, compared to plan without contrast. However, statistical analysis revealed no significant impact (Tab. 2 and 3) on dosimetric plans for minimum, mean and maximum doses of all plans ($p > 0.05$).

Table 2. Comparison of doses calculated from non-contrast and contrast-enhanced computed tomographies (CTs)

	C–			C+			p-value
	Mean	SD	Range	Mean	SD	Range	
D_{max}	70.9464	1.1444	69.146–72.616	70.9739	0.9376	69.745–72.356	0.499
D_{min}	49.9181	10.078	36.598–61.97	50.0213	10.0328	37.463–62.5	0.7353
D_{mean}	66.5869	1.3333	64.684–68.83	66.6586	1.0083	65.49–68.5	0.7353

SD — standard deviation

Table 3. Comparison of doses calculated from non-contrast and contrast enhanced computed tomographies (CTs) with manual regions overriding

	C–			C+ mdf			p-value
	Mean	SD	Range	Mean	SD	Range	
D_{max}	70.9464	1.1444	69.146–72.616	70.9481	0.9406	69.717–72.29	0.74
D_{min}	49.9181	10.0780	36.598–61.97	49.8324	9.95994	37.462–61.71	0.40
D_{mean}	66.5869	1.3333	64.684–68.83	66.6464	1.01442	65.503–68.5	0.61

SD — standard deviation

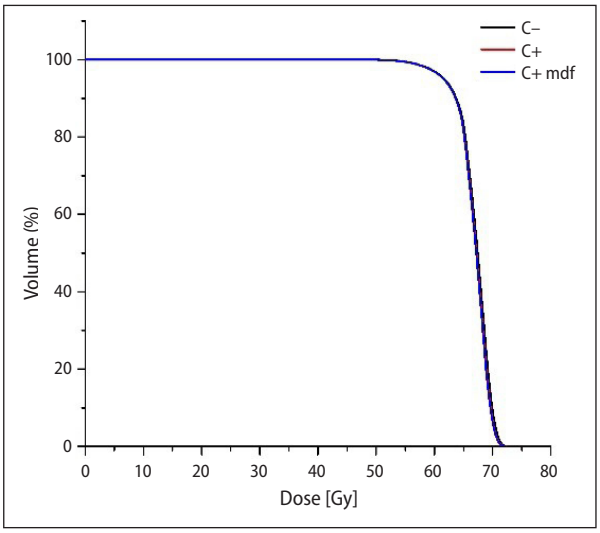

Figure 2. Dose volume histograms (DVHs) comparison of planning target volume (PTV) for dosimetric plans of the three scans for one patient

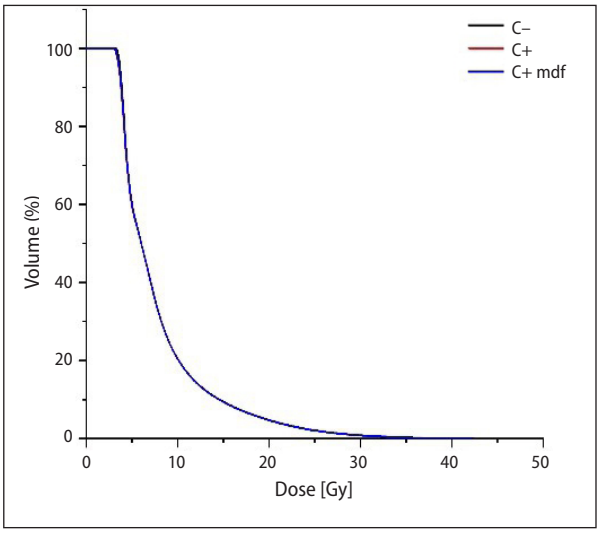

Figure 3. Comparison of spinal cord histograms for dosimetric plans of the three scans for one patient

Moreover, DVHs and maximum doses to the spinal cord and lung volumes that received 20 and 30 Gy (V20 and V30) are calculated and compared for the three scan cases. The results of the comparison are presented in Tables 4 and 5. The differences between the different cases considered are obtained by the Wilcoxon signed rank test.

According to the Wilcoxon test, no significant statistical difference was observed in terms of V20, V30 and mean dose to normal lungs, as well as D_{max} calculated at the spinal cord. Figure 3 illustrates the obtained DVH.

Tables 6–7 recapitulate quality indices for all patients in the three scans. The comparison between the non-contrast plan and other plans showed no

Table 4. Comparison of spinal cord maximum and normal lung doses calculated from non-contrast and contrast-enhanced computed tomographies (CTs)

	C–			C+			p-value
	Mean	SD	Range	Mean	SD	Range	
Normal lung [Gy]	18.3177	5.77355	8.744–22.856	18.3684	4.42839	11.993–22.7	0.61
V20 (%)	30.1107	13.35027	13.071–50.22	29.8625	10.55957	18.25–47.134	0.87
V30 (%)	22.0967	7.72529	12.08–32.728	22.1981	5.86262	15.736–30.01	0.74
Spinal cord D_{max}	40.0617	9.97407	18.81–48.198	40.1724	10.23708	18.48–49.098	0.61

SD — standard deviation

Table 5. Comparison of spinal cord maximum and normal lung doses calculated from non-contrast and contrast-enhanced computed tomographies (CTs) with manual regions overriding

	C–			C+ mdf			p-value
	Mean	SD	Range	Mean	SD	Range	
Normal lung Mean [Gy]	18.3177	5.77355	8.744–22.856	18.3256	4.37785	11.99–22.4	0.87
V20 (%)	30.1107	13.35027	13.071–50.22	29.8367	10.58962	18.25–47.134	0.87
V30 (%)	22.0967	7.72529	12.08–32.728	22.6573	6.42852	15.74–30.023	0.74
Spinal cord D_{max}	40.0617	9.97407	18.81–48.198	40.1777	10.19213	18.6–49.093	0.75

SD — standard deviation

Table 7. Comparison of conformity and homogeneity indices calculated from non-contrast and contrast-enhanced computed tomographies (CTs) with manual regions overriding

	C–			C+mdf			p-value
	Mean	SD	Range	Mean	SD	Range	
CI	1.95	0.67	1.42–3.60	1.95	0.67	1.39–3.60	0.11
HI	1.13	0.15	1.10–1.16	1.12	0.13	1.11–1.15	0.51

SD — standard deviation; CI — conformity index; HI — heterogeneity index

Table 6. Comparison of conformity and homogeneity indices calculated from non-contrast and contrast-enhanced computed tomographies (CTs)

	C–			C+			p-value
	Mean	SD	Range	Mean	SD	Range	
CI	1.95	0.67	1.42–3.60	1.95	0.66	1.39–3.59	0.16
HI	1.13	0.15	1.10–1.16	1.13	0.13	1.11–1.15	0.67

SD — standard deviation; CI — conformity index; HI — heterogeneity index

significant impact of a contrast agent or manual region overriding on the quality plans for CI and HI for all patients.

Discussion

For the purpose of this study, we examined the effects of using intravenous contrast CT scans on dose distribution of lung cancer 3D-RCT treatment plans by comparing doses calculated on non-contrast and contrast enhanced CTs by the same dosimetry plan, and estimating the degree of dose errors.

Based on a potentially remarkable difference in HU values for the heart, which exhibits a structure that will receive irradiation for many cases of patients. We examined the importance of CT Hounsfield number changes on contrast-affected regions and quantify the dosimetry effects of using contrast-enhanced CT scans with a contrast agent in treatment planning.

We also performed an efficiency study of manual correction of HU regions affected by contrast and thus by replacing HU with its average given by non-contrast scanner. To increase the congruence between the two scans as much as possible, a complete analysis of PTV and OAR dose difference is carried out.

Results show that using IV contrast did not lead to clinically significant differences in PTV coverage, OAR dose or Wilcoxon test p-value.

Numerous studies have addressed the impact on radiation dose calculations of using contrast-enhanced CT scans for different locations. For head and neck cancer, it did not result in clinically relevant target dose coverage errors [24–26].

Other studies performed on lung cancer patients showed that the effect of IV contrast on dose calculation for lung cancer treatment was negligible. However, these earlier studies compared and focused only on absolute differences in PTV dose coverage, and not on critical normal organs irradiations [27–29].

In the present study, treatment planning was first made on non-contrast CT images. Then, the plans were copied on contrast-enhanced images, and doses were recalculated. A density correction was made to heart contrast-enhanced on IV contrast-enhanced scans to override possible dose calculation errors that may be caused by contrast-enhanced in the heart.

The results demonstrate that there are no statistically significant differences on dose calculation between plans calculated on the non-contrast and contrast scans, even more on the contrast scan with manual regions overriding.

So, it may not be necessary to consider the presence of IV contrast on dose calculation. This confirms the results of previous researchers in this field [27, 29].

It was indisputable that contrast enhanced scans provided clear target and critical structure projection, while avoiding doubling the patient's dose of radiation caused by the scanner when taking the CT scan and respecting the ALARA (As Low As Reasonably Achievable) radiation safety principle.

Moreover, potential fusion errors are eliminated. Thus, there is no justification for performing two scans, and it will be too desirable to use the IV scan with enhanced contrast for dose calculation.

Conclusion

In summary, the present study indicates that differences in dose calculation between IV-contrast enhanced CT scans and contrast-less scans are not significantly remarkable in the treatment planning for lung cancer. However, recommendations can be made that just one planning CT scan with a contrast agent needs to be taken. That scan will not influence the dose calculations significantly while avoiding useless scans, manually overriding contrast in the contrast-enhanced regions, and user dependent errors that can be caused by scan co-registration for contouring.

This recommendation may prevent patients from performing the scan twice, which may waste time and money. It is important to remember that this practice could prevent double exposure to x-rays emanating from a CT scan.

Conflict of interests

The authors declare that they have no known competing financial interests or personal relationships that could have appeared to influence the work reported in this paper.

Funding

Nothing to disclose.

References

1. Washington CM, Leaver DT. Principles and practice of radiation therapy, 4th ed. Elsevier Mosby, St. Louis 2016.
2. Patz EF, Erasmus JJ, McAdams HP, et al. Lung cancer staging and management: comparison of contrast-enhanced and nonenhanced helical CT of the thorax. Radiology. 1999; 212(1): 56–60, doi: 10.1148/radiology.212.1.r99jl1956, indexed in Pubmed: 10405720.
3. Cascade PN, Gross BH, Kazerooni EA, et al. Variability in the detection of enlarged mediastinal lymph nodes in staging lung cancer: a comparison of contrast-enhanced and unenhanced CT. AJR Am J Roentgenol. 1998; 170(4): 927–931, doi: 10.2214/ajr.170.4.9530036, indexed in Pubmed: 9530036.
4. Takahashi M, Nitta N, Takazakura R, et al. Detection of mediastinal and hilar lymph nodes by 16-row MDCT: is contrast material needed? Eur J Radiol. 2008; 66(2): 287–291, doi: 10.1016/j.ejrad.2007.05.028, indexed in Pubmed: 17628379.
5. Abuhijla F, Al-Mousa A, Abuhijlih R, et al. Variables altering the impact of respiratory gated CT simulation on planning target volume in radiotherapy for lung cancer. Rep Pract Oncol Radiother. 2019; 24(2): 175–179, doi: 10.1016/j.rpor.2019.01.008, indexed in Pubmed: 30814917.
6. Adamczyk M, Kruszyna-Mochalska M, Rucińska A, et al. Software simulation of tumour motion dose effects during flattened and unflattened ITV-based VMAT lung SBRT. Rep Pract Oncol Radiother. 2020; 25(4): 684–691, doi: 10.1016/j.rpor.2020.06.003, indexed in Pubmed: 32581656.
7. Vojtíšek R. Cardiac toxicity of lung cancer radiotherapy. Rep Pract Oncol Radiother. 2020; 25(1): 13–19, doi: 10.1016/j.rpor.2019.10.007, indexed in Pubmed: 31762693.
8. Abdel-Wahab M, Bourque JM, Pynda Y, et al. Status of radiotherapy resources in Africa: an International Atomic Energy Agency analysis. Lancet Oncol. 2013; 14(4): e168–e175, doi: 10.1016/s1470-2045(12)70532-6, indexed in Pubmed: 23561748.
9. Wippold FJ. CT and MR imaging of head and neck cancer. In: Chao KS, Ozyigit G. ed. Intensity modulated radiation therapy for head and neck cancer, 4th ed. Lippincott Williams & Wilkins, Philadelphia : 18–29.
10. Eisbruch A. Head and neck cancer: overview. In: Mundt AJ, Roeske JC. ed. Intensity modulated radiation therapy: a clinical perspective. BC Decker Inc, Ontario 2005: 264–75.
11. Nasrollah J, Mikaeil M, Omid E, et al. Influence of the intravenous contrast media on treatment planning dose calculations of lower esophageal and rectal cancers. J Cancer Res Ther. 2014; 10(1): 147–152, doi: 10.4103/0973-1482.131465, indexed in Pubmed: 24762502.
12. Choi Y, Kim JK, Lee HS, et al. Influence of intravenous contrast agent on dose calculations of intensity modulated radiation therapy plans for head and neck cancer. Radiother Oncol. 2006; 81(2): 158–162, doi: 10.1016/j.radonc.2006.09.010, indexed in Pubmed: 17050020.
13. Wertz H, Jäkel O. Influence of iodine contrast agent on the range of ion beams for radiotherapy. Med Phys. 2004; 31(4): 767–773, doi: 10.1118/1.1650871, indexed in Pubmed: 15124994.
14. Meng Y, Yang H, Wang W, et al. Excluding PTV from lung volume may better predict radiation pneumonitis for intensity modulated radiation therapy in lung cancer patients. Radiat Oncol. 2019; 14(1): 7, doi: 10.1186/s13014-018-1204-x, indexed in Pubmed: 30642354.
15. Shaw E, Kline R, Gillin M, et al. Radiation Therapy Oncology Group: radiosurgery quality assurance guidelines. Int J Radiat Oncol Biol Phys. 1993; 27(5): 1231–1239, doi: 10.1016/0360-3016(93)90548-a, indexed in Pubmed: 8262852.
16. Oulhouq Y, Rrhioua A, Zerfaoui M, et al. Dosimetric Effect Resulting From the Collimator Angle, the Isocenter Move, and the Gantry Angle Errors. Iran J Med Phys. 2019; 16: 355–361.
17. Petrova D, Smickovska S, Lazarevska E. Conformity Index and Homogeneity Index of the Postoperative Whole Breast Radiotherapy. Open Access Maced J Med Sci. 2017; 5(6): 736–739, doi: 10.3889/oamjms.2017.161, indexed in Pubmed: 29123573.
18. Feuvret L, Noël G, Mazeron JJ, et al. Conformity index: a review. Int J Radiat Oncol Biol Phys. 2006; 64(2): 333–342, doi: 10.1016/j.ijrobp.2005.09.028, indexed in Pubmed: 16414369.

19. Guy CL, Weiss E, Che S, et al. Evaluation of Image Registration Accuracy for Tumor and Organs at Risk in the Thorax for Compliance With TG 132 Recommendations. Adv Radiat Oncol. 2019; 4(1): 177–185, doi: 10.1016/j.adro.2018.08.023, indexed in Pubmed: 30706026.
20. Huttenlocher DP, Klanderman GA, Rucklidge WJ. Comparing images using the Hausdorff distance. IEEE Trans Pattern Anal Mach Intell. 1993; 15(9): 850–863, doi: 10.1109/34.232073.
21. Kumarasiri A, Siddiqui F, Liu C, et al. Deformable image registration based automatic CT-to-CT contour propagation for head and neck adaptive radiotherapy in the routine clinical setting. Med Phys. 2014; 41(12): 121712, doi: 10.1118/1.4901409, indexed in Pubmed: 25471959.
22. Fabri D, Zambrano V, Bhatia A, et al. A quantitative comparison of the performance of three deformable registration algorithms in radiotherapy. Z Med Phys. 2013; 23(4): 279–290, doi: 10.1016/j.zemedi.2013.07.006, indexed in Pubmed: 23969092.
23. Scaggion A, Fiandra C, Loi G, et al. Free-to-use DIR solutions in radiotherapy: Benchmark against commercial platforms through a contour-propagation study. Phys Med. 2020; 74: 110–117, doi: 10.1016/j.ejmp.2020.05.011, indexed in Pubmed: 32464468.
24. Liauw SL, Amdur RJ, Mendenhall WM, et al. The effect of intravenous contrast on intensity-modulated radiation therapy dose calculations for head and neck cancer. Am J Clin Oncol. 2005; 28(5): 456–459, doi: 10.1097/01.coc.0000170796.89560.02, indexed in Pubmed: 16199983.
25. Choi Y, Kim JK, Lee HS, et al. Influence of intravenous contrast agent on dose calculations of intensity modulated radiation therapy plans for head and neck cancer. Radiother Oncol. 2006; 81(2): 158–162, doi: 10.1016/j.radonc.2006.09.010, indexed in Pubmed: 17050020.
26. Létourneau D, Finlay M, O'Sullivan B, et al. Lack of influence of intravenous contrast on head and neck IMRT dose distributions. Acta Oncol. 2008; 47(1): 90–94, doi: 10.1080/02841860701418861, indexed in Pubmed: 17934894.
27. Kimlin K, Mitchell J, Knight RT. Effects of iodinated contrast media on radiation therapy dosimetry for pathologies within the thorax. Radiographer. 2013; 53(2): 30–34, doi: 10.1002/j.2051-3909.2006.tb00053.x.
28. Shi W, Liu C, Lu Bo, et al. The effect of intravenous contrast on photon radiation therapy dose calculations for lung cancer. Am J Clin Oncol. 2010; 33(2): 153–156, doi: 10.1097/COC.0b013e3181a44637, indexed in Pubmed: 19806038.
29. Li H, Bottani B, DeWees T, et al. Prospective study evaluating the use of IV contrast on IMRT treatment planning for lung cancer. Med Phys. 2014; 41(3): 031708, doi: 10.1118/1.4865766, indexed in Pubmed: 24593712.